

Bestimmung des Windkanal-Turbulenzgrades mittels PIV/PTV

Estimating wind tunnel turbulence level by means of PIV/PTV

Sven Scharnowski, Matthew Bross and Christian J. Kähler

Institut für Strömungsmechanik und Aerodynamik, Universität der Bundeswehr München, Werner-Heisenberg-Weg 39, 85577 Neubiberg

Schlagworte: Turbulenzgrad, Messunsicherheit

Key words: Turbulence level, Measurement Uncertainty

Abstract

This work analyzes the free-stream flow of the trisonic wind tunnel Munich (TWM) by means of particle image velocimetry (PIV) and Particle Tracking Velocimetry (PTV). The goal is to determine the flow quality, e.g. the turbulence level, over the operating range of the facility. The capability of PIV/PTV for the estimation of small velocity fluctuations is investigated in detail. It is shown that a small field of view of $26\text{ mm} \times 22\text{ mm}$ in combination with a large particle image displacement of 100 pixel allows for precise velocity measurements. Furthermore, a variation of the time separation between the PIV double images, Δt , enables the measurement uncertainty to be determined, which was estimated to be as low as 0.04% for a mean displacement of $\Delta x = 100$ pixel and an interrogation window size of 32×32 pixel. Regarding the wind tunnel turbulence, it was found that the turbulence level generally decreases with increasing Mach number, starting with 1.9% at $Ma = 0.3$ and reaching 0.45% at $Ma = 3.0$.

Introduction

The quantification of the turbulence level of a wind tunnel is an important part of any measurement results. It completes the actual measurement data and allows measurements at different facilities to be compared and can be used to set the inflow conditions for numerical simulations. The turbulence level Tu is usually described by the standard deviation of the fluctuations of the streamwise velocity component normalized by the mean streamwise velocity

$$Tu = \frac{\sqrt{\langle u'^2 \rangle}}{\langle u \rangle} \quad (1)$$

where the standard deviation is computed from the ensemble of velocity measurements

$$\sqrt{\langle u'^2 \rangle} = \sqrt{\frac{1}{N} \sum_n (u_n - \langle u \rangle)^2} \quad (2)$$

with $\langle u \rangle$ being the mean velocity.

Accurate turbulence measurements require a measurement system that has an uncertainty that is well below the velocity fluctuations of interest. Additionally, the measurement volume from that each velocity vector is estimated must be small compared to the turbulent structures. Hot-wire probes are well suited for precise velocity measurements with high temporal resolution (Hutchins et al. 2009, Hultmark et al. 2013). However, they have the drawback that they are intrusive and that extracting the velocity from the measured signal requires knowledge about the flow density. Furthermore, at supersonic Mach numbers also shock waves generated by the probe bias the measurements. Therefore the application of hot-wire probes is usually limited to incompressible flow. A non-intrusive alternative measurement technique is the Laser-Doppler velocimetry (LDV) (George & Lumley 1973, Shirai et al. 2006). Due to its working principle LDV does not require knowledge about the flow density and is therefore suited for measurements in compressible flows. Hot-wire probe and LDV are measurement techniques with the capability of high temporal resolution however, they only provide point wise information about the flow. In order to analyze the spatial organization of turbulent structures planar or volumetric measurement techniques are needed. Particle image velocimetry (PIV) and particle tracking velocimetry (PTV) provide such spatial information but are known to have higher measurement uncertainties than hot-wire probes and LDV.

The aim of this work is to investigate the capability of PIV/PTV to estimate the wind tunnel turbulence levels. Since velocity fluctuations on the order of 1% are expected, the measurement uncertainty should be well below that value. In order to ensure highly accurate measurements with PIV/PTV the time separation between the double images Δt must be optimized. On the one hand, the particle image displacement on the camera sensor must be large to achieve low relative uncertainty (Scharnowski & Kähler, 2016a). On the other hand, the particle displacement on the physical plane must be small to avoid loss-of-pairs due to out-of-plane motion as well as filtering effects due to gradients (Scharnowski & Kähler, 2013). In the case of PIV/PTV, the measured displacement fluctuations $\Delta x' = \Delta x - \langle \Delta x \rangle$ are a combination of the actual velocity fluctuations $u' = u - \langle u \rangle$ and the random error of the displacement measurement, characterized by its standard deviation $\sigma_{\Delta x}$

$$\langle \Delta x'^2 \rangle = \Delta x^2 \cdot \langle \Delta x'^2 \rangle / \langle \Delta x \rangle^2 + \sigma_{\Delta x}^2 = \Delta x^2 \cdot Tu^2 + \sigma_{\Delta x}^2 \quad (3)$$

In order to perform reliable turbulence level estimations by means of PIV/PTV, the measurement setup and the evaluation procedure must be selected carefully to ensure low measurement uncertainty.

In the following the test facility, the measurement setup and the data evaluation are described in detail. Further on, a carefully study of the effect of the particle image displacement and the interrogation window size on the estimated turbulence level is carried out. Finally, conclusions are drawn from the presented results.

Measurement Setup

The measurements were performed in the trisonic wind tunnel at the Bundeswehr University in Munich (TWM). The TWM facility is a blow-down type wind tunnel with a 300 mm wide and 675 mm high test section. Two adjustable throats, the Laval nozzle upstream of the test section and the diffusor further downstream, enable an operating range of Mach numbers from 0.2 to 3.0. The facility has two tanks that can be pressurized up to 20 bar above ambient

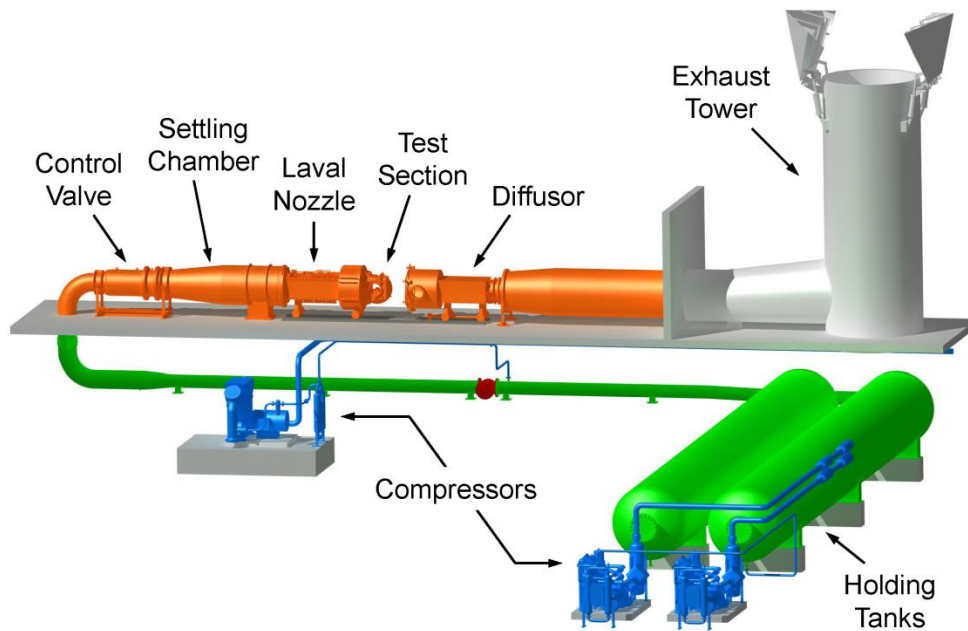


Fig. 1 Sketch of the trisonic wind tunnel Munich

pressure, holding a total volume of 356 m³ of dry air. To control the Reynolds number, the total pressure in the test section is varied between 1.2 to 5 bar. The facility is discussed in detail in Bolgar et al. 2018. A sketch of the wind tunnel is shown in Fig. 1.

For the PIV measurements, the flow was seeded with Di-Ethyl-Hexyl-Sebacat (DEHS) tracer particles with a mean diameter of 1 μm, as described by Kähler et al. 2002. The tracers were illuminated by a 500 μm thick light sheet in a horizontal plane at the center of the test section. The scattered light of the seeding droplets was imaged onto the sensor of a sCMOS camera with double image capability and global shutter by means of a 100 mm lens in combined with a 2× tele converter. The resulting size of the field of view is 26 mm×22 mm and the resulting scaling factor is 10.4 μm/pixel.

With this PIV setup, a mean particle image diameter of about 3.4 pixel was achieved. From the autocorrelation function of the images a background noise level with a standard deviation of about 50 counts was estimated with the method presented in Scharnowski et al. 2016b. This noise level leads to a loss-of-correlation due to image noise of $F_c \approx 0.91$ and to a signal-to-noise ratio of $SNR \approx 3.2$, which is considered to be well suited for accurate PIV evaluation.

In order to analyze the effect of the time between the double images Δt and the interrogation window size D_I on the estimated turbulence level, these parameters were varied for a Mach number of $Ma = 0.3$ and a total pressure of $p_0 = 1.5$ bar. After checking that about 250 double images acquired at 15 Hz lead to converged results, 1000 double images were recorded for nine different Δt between 0.2 μs and 20 μs, corresponding to a mean particle image shift between $\Delta x \approx 2$ pixel and 200 pixel. The PIV recordings were evaluated using state-of-the-art PIV software including multi-pass image deformation and Gaussian window weighting. The final window size was varied between 12×12 pixel and 64×64 pixel.

Particle tracking velocimetry (PTV) was also applied to the data set as a comparison to the PIV calculations. In order to track pairs of particle images, the 2D locations of the particle images in the field of view must be identified. This is accomplished by applying 2D Gaussian fitting function to the particle images, rejecting particle images that exceed a defined intensity

threshold or min/max pixel size. The tracking of corresponding particle image pairs is then done by applying a non-iterative double frame particle tracking approach (Fuchs et al. 2017). To remove spurious results, an outlier detection is applied that compares neighboring tracks and rejecting ones that are more than a defined threshold. Finally a Gaussian fit is applied to all the double frame tracks and only values within 2σ are considered for the mean and standard deviation calculations shown in the results.

Results and Discussions

The results for the variation of the particle image shift Δx and different interrogation window sizes D_1 are illustrated in Fig. 2 by means of example velocity fields. For each column in the figure the same PIV recordings were evaluated. It can be seen from the top left image in the figure, that with decreasing displacements and decreasing interrogation window size the noise is amplified. It is obvious that under these conditions the measurement uncertainty is too high to reliably estimate the velocity fluctuations. For increased Δx as well as for increased D_1 the vector fields look much smoother and are therefore better suited for turbulence level estimations. The fields are less noisy because the uncertainty of the estimated velocity is reduced by the decreased uncertainty of the particle image displacement $\sigma_{\Delta x}$ (in the case of larger D_1) or by enlarged mean displacement $\langle \Delta x \rangle$. However, care must be taken when increasing Δx or D_1 for two reasons. First, the larger the particle image displacement becomes the higher the risk of introducing bias errors is due to curved streamlines, which are not captured in double-pulse PIV experiments (Scharnowski & Kähler, 2013). Second, larger interrogation windows causes increased spatial low-pass filtering of the velocity field, leading to smoothed results which might filter out small scale turbulent structures (Scharnowski et al., 2012). To minimize these two effects, a small field of view was selected such that the interrogation window sizes as well as the particle image displacement are small projected on the measurement plane.

To further analyze the effect of Δx and D_1 , Fig. 3 illustrates the standard deviation of the shift vector fluctuations with respect to the mean particle image shift for different window sizes. For comparison PTV results are also shown. The symbols in the figure represent the spatial mean of the temporal standard deviation and the error bars correspond to the spatial variations within the field of view. The dashed lines indicate the distribution of a fit-function using Eq. (3). Values for the fit-parameters Tu and $\sigma_{\Delta x}$ are given in the figure. As expected, the estimated turbulence level increases with decreasing interrogation window size indicating that some of the turbulent structures are smaller than the interrogation windows. However, since the changes in the Tu values are very small it can be concluded that most structures are larger than 64 pixel ($= 670 \mu\text{m}$). Furthermore, the PTV results, which do not suffer from spatial low-pass filtering, confirm the PIV results of the smallest tested interrogation windows. Besides the turbulence level, the fitting parameters in Fig. 3 also provide the measurement uncertainty $\sigma_{\Delta x}$. As expected the measurement uncertainty increases with decreasing window size. For PTV $\sigma_{\Delta x}$ is slightly larger than for PIV. This is because only one particle image pair is used for computing each vector and the particle image shift must be evaluated by using a fit-function twice to detect both particle image positions.

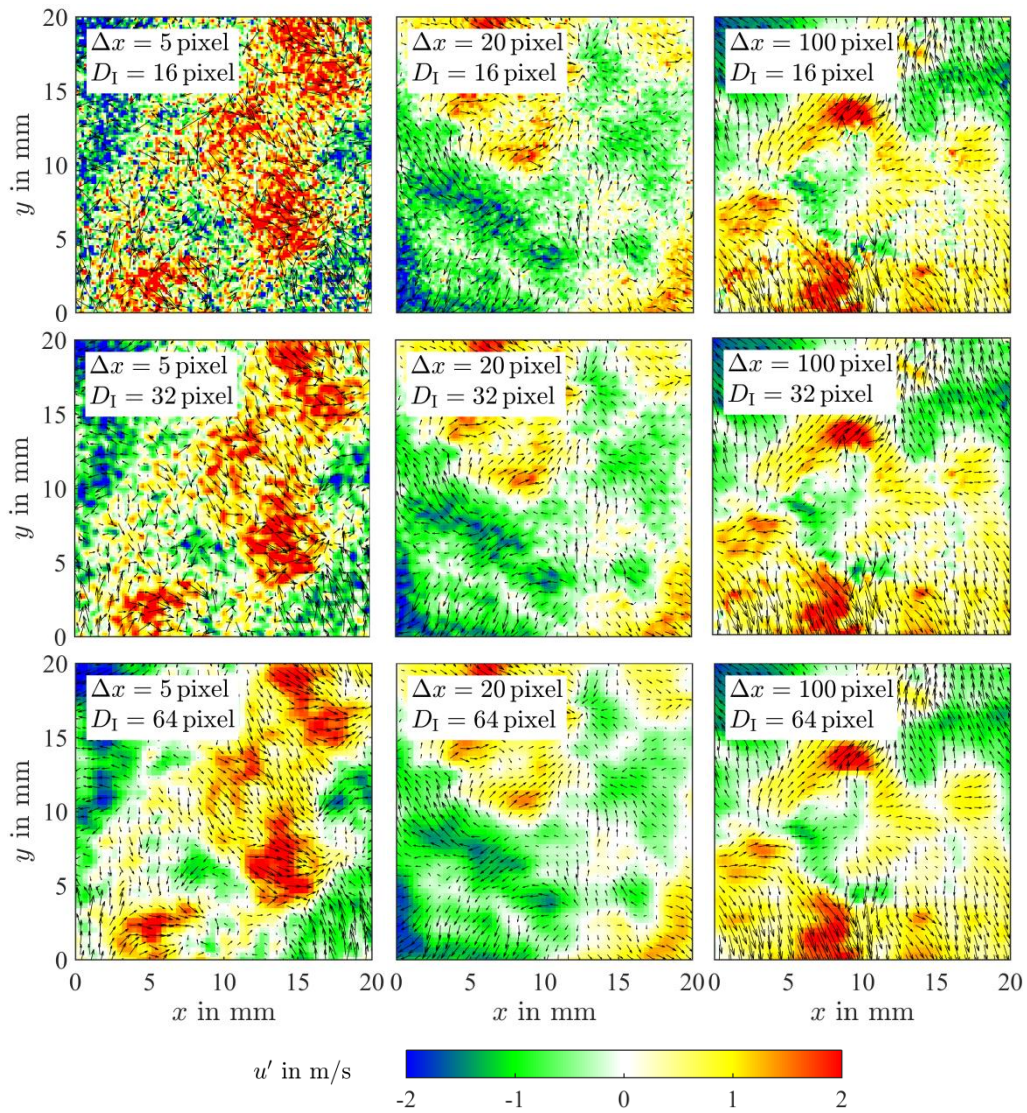


Fig. 2 Example velocity fields for a Mach number of $M = 0.3$ and a total pressure of $p_0 = 1.5$ bar computed from PIV recordings with different particle image displacements Δx (increasing from left to right) and different interrogation window sizes D_I (increasing from top to bottom).

Another important error source that must be considered for PIV and PTV measurements is the so-called peak locking effect. Peak locking is a bias error that shifts the estimated displacement values towards the next integer pixel positions and is caused by too small particle images. In the case of peak locking the probability density function of the displacement shows peaks at integer pixel values (Christensen, 2004). As a result, the velocity distribution would change with varying particle image displacement. However, looking at the probability density function of the measured velocity fluctuations in Fig. 4, such phenomena cannot be observed. All the tested particle images displacements result in smooth histograms without multiple peaks. The differences in the width of the distributions are caused by the varying particle image shifts, which affect the estimated velocity fluctuations according to Eq. (3).

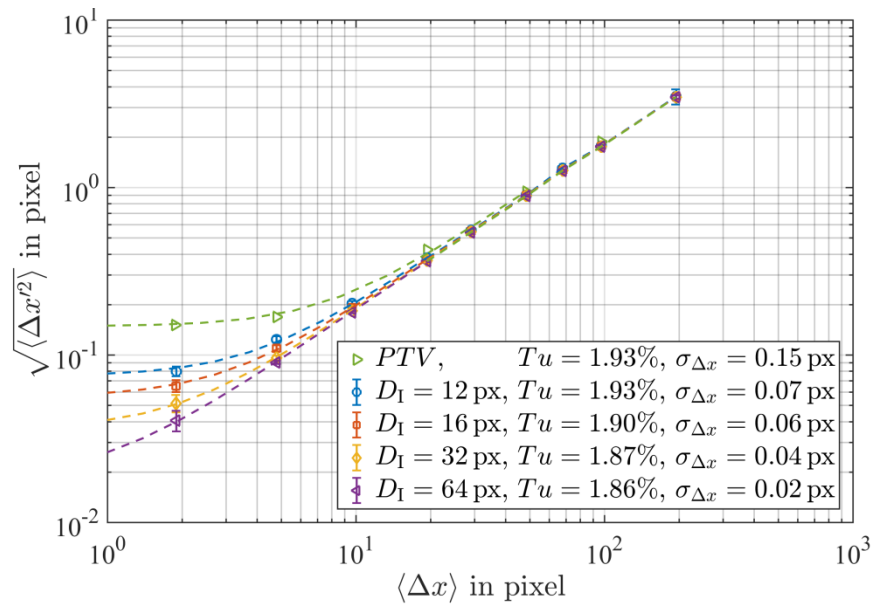


Fig. 3 Measured displacement fluctuations as a function of the mean particle image shift for different PIV interrogation windows and for PTV. The dashed curves represent fit-functions according to Eq. (3).

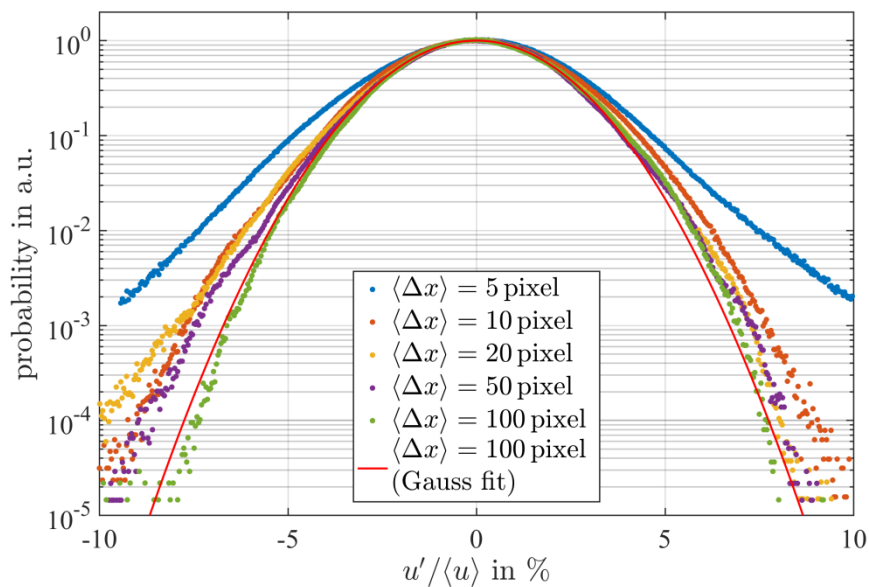


Fig. 4 Histogram of the velocity fluctuations determined from varying particle image shifts.

Based on the presented sensitivity analysis, the parameters for a reliable estimation of the wind tunnel turbulence level over the full range of possible Mach numbers and Reynolds numbers were selected. In order to minimize the wind tunnel run time, only one run with 500 densely seeded image pairs and a particle image shift of $\Delta x \approx 100$ pixel was performed for each wind tunnel condition. Due to the slightly higher measurement uncertainty of PTV at densely seeded flows it was decided to use PIV for further evaluation. Alternatively, lower seeded images could be evaluated with PTV but in order to reach the same statistical convergence of the higher seeded flow more wind tunnel blow downs (and refills) would be needed. The PIV images were evaluated with a final interrogation window size of $D_1 = 32$ pixel. The resulting turbulence levels are shown in Fig. 5. It can be clearly seen from the fig-

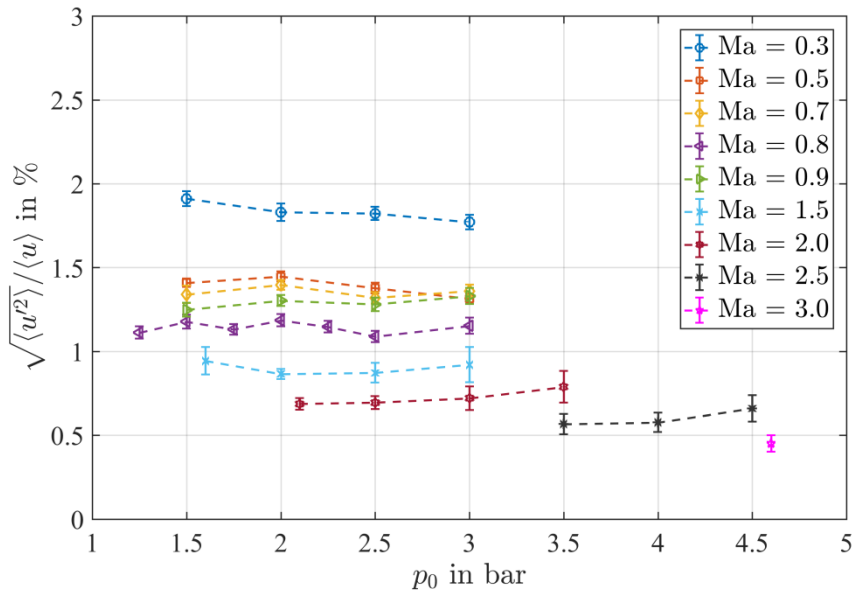


Fig. 5 Wind tunnel turbulence level over the working range of the TWM facility.

ure that the total pressure p_0 and thus the Reynolds number have only a minor effect on the velocity fluctuations. However, the Mach number clearly influences the turbulence level. With the exception of $Ma = 0.9$ the turbulence level decreases monotonically with increasing Mach number and reaches a value of $Tu = 0.45\%$ for $Ma = 3.0$.

Conclusions

It can be concluded that PIV and PTV are well suited to reliably estimate wind tunnel turbulence levels under the following conditions:

- The PIV interrogation window size D_1 projected on the measurement plane must be small compared to the dominant turbulent structures. Otherwise the application of PTV is recommended.
- The particle image displacement Δx must be large on the image plane to reduce the relative uncertainty.
- The particle displacement on the measurement plane must be small to avoid bias errors due to velocity gradients, which means the magnification must be sufficiently large.
- A variation of the particle image displacement Δx allows the measurement uncertainty to be determined.
- A variation of the interrogation window size D_1 allows bias errors due to spatial filtering to be detected.

Thus, for accurate PIV/PTV measurements it is recommended to use camera sensors with large number of pixels or multiple cameras which allow for high resolution and large dynamic spatial range at the same time, as demonstrated by Curvier et al. 2017. Finally, a variation of Δx and D_1 provides information about the reliability of the results.

Acknowledgment

This work is supported by the Priority Programme SPP 1881 Turbulent Superstructures of the Deutsche Forschungsgemeinschaft.

References

- Bolgar, I., Scharnowski, S., Kähler, C.J., 2018:** „The Effect of the Mach Number on a Turbulent Backward-Facing Step Flow”, *Flow, Turbulence and Combustion*, Vol. 1, No. 28
- Christensen, K.T., 2004:** “The influence of peak-locking errors on turbulence statistics computed from PIV ensembles”, *Experiments in Fluids*, Vol. 36, No. 3, pp. 484–497
- Cuvier, C., Srinath, S., Stanislas, M., Foucaut, J. M., Laval, J. P., Kähler, C. J., Hain, R., Scharnowski, S., Schröder, A., Geisler, R., Agocs, J., Röse, A., Willert, C., Klinner, J., Amili, O., Atkinson, C., Soria, J., 2017:** “Extensive characterisation of a high Reynolds number decelerating boundary layer using advanced optical metrology”, *Journal of Turbulence*, Vol. 18, No. 10, pp. 929–972
- George, W.K., Lumley, J.L., 1973:** “The laser-Doppler velocimeter and its application to the measurement of turbulence”, *Journal of Fluid Mechanics*, Vol. 60, No. 2, pp. 321–362
- Fuchs, T., Hain, R., Kähler, C.J., 2017:** “Non-iterative double-frame 2D/3D particle tracking velocimetry”, *Experiments in Fluids*, Vol. 58, No. 9, pp. 119
- Hultmark, M., Vallikivi, M., Bailey, S.C.C., Smits, A.J., 2013:** “Logarithmic scaling of turbulence in smooth- and rough-wall pipe flow”, *Journal of Fluid Mechanics*, Vol. 728, pp. 376–395
- Hutchins, N., Nickels, T.B., Marusic, I. & Chong, M.S., 2009:** “Hot-wire spatial resolution issues in wall-bounded turbulence”, *Journal of Fluid Mechanics*, Vol. 635, pp. 103–136
- Kähler, C.J., Sammler, B., Kompenhans, J., 2002:** “Generation and control of tracer particles for optical flow investigations in air”, *Experiments in fluids*, Vol. 33, No. 6, pp. 736–742
- Scharnowski, S., Hain, R., Kähler, C.J., 2012:** „Reynolds stress estimation up to single-pixel resolution using PIV-measurements”, *Experiments in fluids*, Vol. 52, No. 4, pp. 985–1002
- Scharnowski, S., Kähler, C.J., 2013:** “On the effect of curved streamlines on the accuracy of PIV vector fields”, *Experiments in Fluids*, Vol. 54, No. 1, pp. 1435
- Scharnowski, S., Kähler, C.J., 2016a:** „Estimation and optimization of loss-of-pair uncertainties based on PIV correlation functions”, *Experiments in Fluids*, Vol. 57, No. 2, pp. 23
- Scharnowski, S., Kähler, C.J., 2016b:** „On the loss-of-correlation due to PIV image noise”, *Experiments in Fluids*, Vol. 57, No. 7, pp. 119
- Shirai, K., Pfister, T., Büttner, L., Czarske, J., Müller, H., Becker, S., Lienhart, H., Durst, F., 2006:** “Highly spatially resolved velocity measurements of a turbulent channel flow by a fiber-optic heterodyne laser-Doppler velocity-profile sensor”, *Experiments in Fluids*, Vol. 40, pp. 473–481